Computational Bounds to Light–Matter Interactions via Local Conservation Laws

Zeyu Kuang and Owen D. Miller
Department of Applied Physics and Energy Sciences Institute, Yale University, New Haven, Connecticut 06511, USA

(Received 31 August 2020; accepted 7 December 2020; published 31 December 2020)

We develop a computational framework for identifying bounds to light–matter interactions, originating from polarization-current-based formulations of local conservation laws embedded in Maxwell's equations. We propose an iterative method for imposing only the maximally violated constraints, enabling rapid convergence to global bounds. Our framework can identify bounds to the minimum size of any scatterer that encodes a specific linear operator, given only its material properties, as we demonstrate for the optical computation of a discrete Fourier transform. It further resolves bounds on far-field scattering properties over any arbitrary bandwidth, where previous bounds diverge.

DOI: 10.1103/PhysRevLett.125.263607

Nanoscale fabrication techniques, computational inverse design [1–4], and fields from silicon photonics [5–8] to metasurface optics [9–12] are enabling transformative use of an unprecedented number of structural degrees of freedom in nanophotonics. An emerging critical need is an understanding of fundamental limits to what is possible, analogous to Shannon's bounds for digital communications [13,14]. In this Letter, we identify an infinite set of local conservation laws that can form the foundation of a general framework for computational bounds to light–matter interactions. We show that this framework enables calculations of bounds for two pivotal applications, for which all previous approaches yield trivial (e.g., divergent) bounds. First, we identify computational bounds on the minimum size of a scatterer encoding any linear operator, demonstrated for an analog optical discrete Fourier transform (DFT). Second, we identify bounds on maximum far-field extinction over any bandwidth, resolving an important gap in power–bandwidth limits [15]. The local power-conservation laws identified here have immediate ramifications across nanophotonics; more generally, they appear to be extensible to linear partial differential equations across physics.

Bounds, or fundamental limits, identify what is possible in a complex design space. Beyond Shannon's bounds, well-known examples include the Carnot efficiency limit [16], the Shockley–Queisser bounds in photovoltaics [17], the Bergman–Milton bounds in the theory of composites [18–20], and the Wheeler–Chu bounds on antenna quality factor [21,22], among many more. In electromagnetism, for a long period of time there were very few bounds on general response functions (with a notable exception being sum rules on total response [23–26]), seemingly due to the complex and nonconvex nature of Maxwell's equations. Yet a flurry of recent results have suggested the possibility for general bounds [15,27–42], for quantities ranging from single-frequency scattering to radiation loss of free electrons, for bulk and 2D materials. Underlying all of these results is one or two energy-conservation laws, arising in various formulations of Maxwell's equations. Additional bounds have been identified via Lagrangian duality [43,44] or physical approximations [45–47]. Yet there are pivotal applications for which all of these approaches either do not apply or offer trivial bounds.

Here we identify an infinite set of conservation laws that must be satisfied by any solution of Maxwell's equations. These laws are "domain oblivious"; i.e., once a designable region is specified, the constraints are valid for *any* possible geometric structure in that region. Moreover, each conservation law is a quadratic form that is amenable to semidefinite relaxation [48,49]. To accelerate the bound computations we develop an algorithm that automatically selects ideal constraints to impose. These bounds lack the intuition of analytical expressions, but they can provide significantly tighter limits.

Local conservation laws.—To start, we derive local conservation laws that must be satisfied by any Maxwell solution. These conservation laws manifest the complex Poynting theorem [50] over any subdomain of a scatterer, but only when formulated in terms of induced polarization currents do they exhibit properties that enable global bounds. We consider any scattering problem comprising arbitrary sources and arbitrary electric and/or magnetic material properties. We use six-vector notation, concatenating electric and magnetic three-vectors for more concise expressions; for example, the electromagnetic fields ψ and polarization currents ϕ are given by $\psi = \begin{pmatrix}\mathbf{E}\\ \mathbf{H}\end{pmatrix}$ and $\phi = \begin{pmatrix}\mathbf{P}\\ \mathbf{M}\end{pmatrix}$, and we use dimensionless units in which the speed of light is 1.

Physically, the conservation laws that form the foundation of our bounds arise from the complex Poynting theorem [50]. As depicted in Fig. 1, Poynting's theorem must apply not only globally over an entire scatterer, but also locally at any point within. We can rewrite the usual Poynting theorem (a function of the electromagnetic fields)

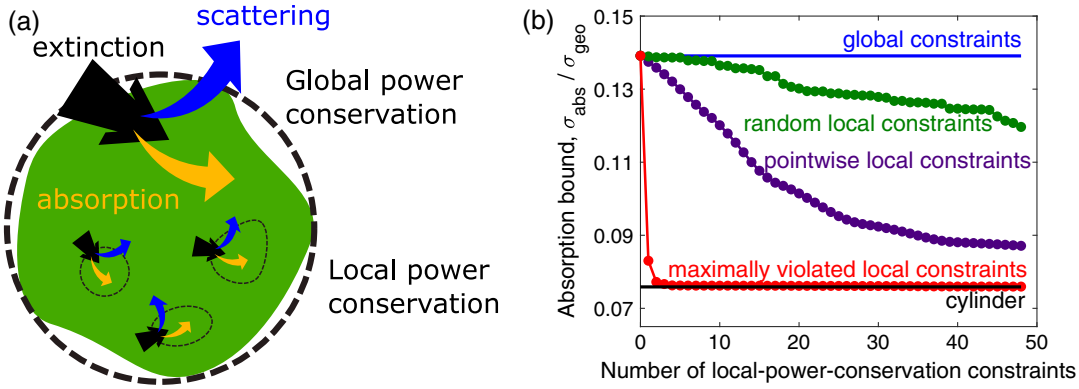

FIG. 1. (a) A freeform, homogeneous photonic scatterer within a designable region (outer dashed circle). Previous bounds utilized global conservation laws (large arrows). Here, we introduce a polarization-current-based formulation of local conservation laws that provide an infinite set of constraints for the identification of global bounds to light–matter interactions. (b) Example of local constraints (green, purple, red) tightening bounds from global constraints only (blue), for maximum absorption from a material with permittivity $\varepsilon = 12 + 0.1i$ in a region with diameter $d = 0.18\lambda$. Our iterative method of selecting maximally violated constraints rapidly converges.

in terms solely of the polarization currents ϕ induced across the scatterer. Ignoring reactive power momentarily, and considering only real power flow, the statement that at any point x the local extinction must equal local absorption plus scattered power can be written:

$$-\frac{\omega}{2}\mathrm{Im}[\phi^\dagger(x)\psi_{\mathrm{inc}}(x)] = \frac{\omega}{2}\phi^\dagger(x)\mathrm{Im}[-\chi^{-1}]\phi(x) + \frac{\omega}{2}\mathrm{Im}\left[\phi^\dagger(x)\int_V \Gamma_0(x,x')\phi(x')dx'\right], \tag{1}$$

where the first term corresponds to extinction, the second term to absorption, and the last term to scattered power. Equation (1) is the well-known optical theorem [50–52], applied to an infinitesimal bounding sphere at point x. We can generalize this expression in three ways, physically argued here and rigorously justified in the Supplemental Material (SM) [53]. First, we can allow for a complex-valued frequency and replace ω with its conjugate ω^*, which makes no difference at real frequencies but will be useful for bandwidth-averaged scattering below. Second, we can remove the imaginary part from Eq. (1), which then manifests the complex Poynting theorem, including reactive power conservation. Finally, instead of considering only a single position x, we can consider any linear combination of points as determined by taking the integral of Eq. (1) against a weighting tensor $\mathbb{D}(x)$ (which also isolates the polarization directions). Taken together, these generalizations comprise the constraints

$$-\frac{\omega^*}{2}\int_V \phi^\dagger(x)\mathbb{D}(x)\psi_{\mathrm{inc}}(x)dx = \frac{\omega^*}{2}\int_V \phi^\dagger(x)\mathbb{D}(x)dx\left[\int_V \Gamma_0(x,x')\phi(x')dx' - \chi^{-1}\phi(x)\right]. \tag{2}$$

Roughly speaking, Eq. (2) represents a linear combination of pointwise equalities from the complex Poynting theorem. To illuminate the algebraic structure of Eq. (2), we can strip away the integrals and position dependencies by assuming any standard numerical discretization [62], in which case ϕ and ψ_{inc} become vectors and $\mathbb{D}$, Γ_0, and χ are matrices. After discretization, Eq. (2) is given in matrix notation by

$$\frac{\omega^*}{2}\phi^\dagger\mathbb{D}\Gamma_0\phi - \frac{\omega^*}{2}\phi^\dagger\mathbb{D}\chi^{-1}\phi = -\frac{\omega^*}{2}\phi^\dagger\mathbb{D}\psi_{\mathrm{inc}}. \tag{3}$$

The complex-Poynting-theorem-based conservation laws of Eqs. (2) and (3) satisfy two key properties that enable global bounds over all possible designs. First, they are domain oblivious: within a designable region, Eqs. (1)–(3) must apply at every point regardless of whether it is part of the scattering domain or the background. Second, they are quadratic forms of the polarization currents, and therefore amenable to semidefinite programming, as we discuss below.

Computational bounds.—Any electromagnetic power- or momentum-flow objective function f will be a linear or quadratic real-valued function of the polarization currents ϕ, which in our matrix notation can be written as $f(\phi) = \phi^\dagger\mathbb{A}\phi + \mathrm{Re}(\beta^\dagger\phi) + c$, where $\mathbb{A}$ is any Hermitian matrix and β and c are any vector and constant, respectively. To identify bounds for any objective f, we replace the Maxwell equation constraint (which is not domain oblivious) with a finite number of constraints of the form of Eq. (3), each with a unique $\mathbb{D}$ matrix given by $\mathbb{D}_j$ for the jth constraint. Then, a bound on the maximum achievable f is given by the solution of

$$\underset{\phi}{\text{maximize}}\ f(\phi) = \phi^\dagger\mathbb{A}\phi + \mathrm{Re}(\beta^\dagger\phi) + c \quad \text{such that } \phi^\dagger\mathrm{Re}\{\mathbb{D}_j\omega^*(\Gamma_0 - \chi^{-1})\}\phi = -\mathrm{Re}(\omega^*\phi^\dagger\mathbb{D}_j\psi_{\mathrm{inc}}). \tag{4}$$

The domain of the optimization variable ϕ is the space of coefficients of the basis functions extending over an entire designable region [e.g., the dashed circled cylinder in Fig. 1(a)]. We have taken only the real part of Eq. (2) because $\mathbb{D} \to i\mathbb{D}$ accounts for the imaginary part. Equation (4) is a key result: it is a formulation of maximum response, subject to all possible local-power conservation laws, as a quadratically constraint quadratic program, i.e., a QCQP optimization problem [49,63]. By virtue of the domain-oblivious property of the constraints, it applies to all possible designs within the designable domain. A bound on the solution of Eq. (4) can be found by standard techniques that relax the original, quadratic program to a higher-dimensional linear program over semidefinite matrices, i.e., a semidefinite program [48,49], which can be solved by interior-point methods [63,64]. Such transformations of QCQPs have led to meaningful bounds in many areas of engineering [49,64–68]; we leave the details of the transformation of Eq. (4) to the SM [53]. The final solution represents a global, unsurpassable bound for any electromagnetic scattering response.

It is computationally prohibitive to impose the infinitely many constraints of Eq. (2). We propose an iterative algorithm for identifying which subset of constraints to use. One should start with the two $\mathbb{D}$ matrices that correspond to global power conservation, i.e., the identity tensor and the identity tensor multiplied by i, which correspond to reactive- and real-power conservation, respectively. (The latter leads to a positive semidefinite quadratic form and is crucial to restricting the magnitude of the solutions.) As a first iteration, we use only those two $\mathbb{D}$ matrices to find an initial bound for Eq. (4), as well as the first-iteration optimal polarization currents, $\phi_{\mathrm{opt},1}$. From those currents, we can identify out of all possible remaining $\mathbb{D}$-matrix constraints which ones are "most violated" by $\phi_{\mathrm{opt},1}$, i.e., which constraint is farthest from zero (under the L_2 norm). The constraint for the corresponding $\mathbb{D}$ matrix is then added to the constraint set, and a second iteration is run, identifying new bounds and new optimal polarization currents. This process proceeds iteratively until convergence. Straightforward linear algebra shows (cf. SM [53]) that after iteration j, with optimal currents ϕ_j, the next constraint to add is the one with $\mathbb{D}$ matrix,

$$\mathbb{D}_{j+1} = \omega \mathrm{diag}[\phi_{\mathrm{opt,j}} \phi_{\mathrm{opt,j}}^{\dagger} (\Gamma_0 - \chi^{-1})^{\dagger} + \phi_{\mathrm{opt,j}} \psi_{\mathrm{inc}}], \quad (5)$$

where "diag" is the diagonal (in space) matrix comprising the diagonal elements of its matrix argument. Figure 1(b) demonstrates the utility of this method of maximally violated constraints for bounding the TE absorption cross section σ_{abs} of a dielectric scatterer of any shape occupying a wavelength-scale cylindrical design region. The designable region need not be symmetric; in the SM [53] we include an example with a triangular region. Whereas the global constraints (blue) are significantly larger than the response of a cylindrical scatterer (black), including local constraints shows that one can clearly identify tighter bounds. Yet both randomly chosen $\mathbb{D}$ matrices (green) and spatially pointwise, delta-function-based $\mathbb{D}$ matrices (purple) show slow convergence. The iterative method via maximally violated constraints shows rapid convergence, requiring only two local constraints. The spatial patterns of both the optimal current distribution and local constraints are shown in the SM [53]. From this method we can clearly identify the cylinder as a globally optimal structure for that material and design region.

S-matrix feasibility.—To demonstrate the power of this framework, we consider a fundamental question in the fields of analog optical computing [69–73] and metasurfaces [9–11]: what is the minimum size of a scatterer that achieves a desired scattering matrix S_{target}? A generic setup is depicted in Fig. 2(a). The target S matrix could manifest lens focusing or metaoptical computing, for example. The objective, then, is to minimize the relative difference between the achievable and target S matrices, i.e., $f_{\mathrm{obj}} = \|S - S_{\mathrm{target}}\|^2 / \|S_{\mathrm{target}}\|^2$, where $\|\cdot\|$ denotes the Frobenius norm. It is straightforward to write this objective in the form appearing in Eq. (4), as the S matrix elements are linear in the polarization currents and the objective is a quadratic form (cf. SM [53]). Then, to determine the minimum feasible size for implementing S_{target}, we can compute the bound on the smallest error between S and S_{target}, and define an acceptable-accuracy threshold (1%) below which the device exhibits the desired functionality with sufficient fidelity.

We apply our framework to two such problems, both of which comprise two-dimensional, nonmagnetic scatterers with refractive index $n = \sqrt{12}$, discretized by the discrete dipole approximation [74,75]. In the first, we identify the smallest domain within which a scatterer can possibly act as a discrete Fourier transform operator over three TE cylindrical-wave channels (cf. SM [53]). The DFT is the foundation for discrete Fourier analysis and many other practical applications [76]. With uniform frequencies and nonuniform sample points t_1, t_2, and t_3 (and t_1 is fixed as a reference to be $t_1 = 0$), a target S matrix that acts as a DFT can be represented as [77]

$$S_{\mathrm{target}}(t_2, t_3) = \frac{1}{\sqrt{3}} \begin{pmatrix} 1 & 1 & 1 \\ 1 & e^{-2\pi i t_2/3} & e^{-2\pi i t_3/3} \\ 1 & e^{-4\pi i t_2/3} & e^{-4\pi i t_3/3} \end{pmatrix}. \quad (6)$$

Figure 2(b) shows the bound-based feasibility map for implementing such an S matrix. Each point in the grid represents a unique DFT matrix (prescribed by the values of t_2 and t_3), and the color indicates the smallest diameter d, relative to wave number k, of a structure that can possibly exhibit the desired DFT-based scattering matrix (at 99% fidelity). There is no structure, with any type of patterning,

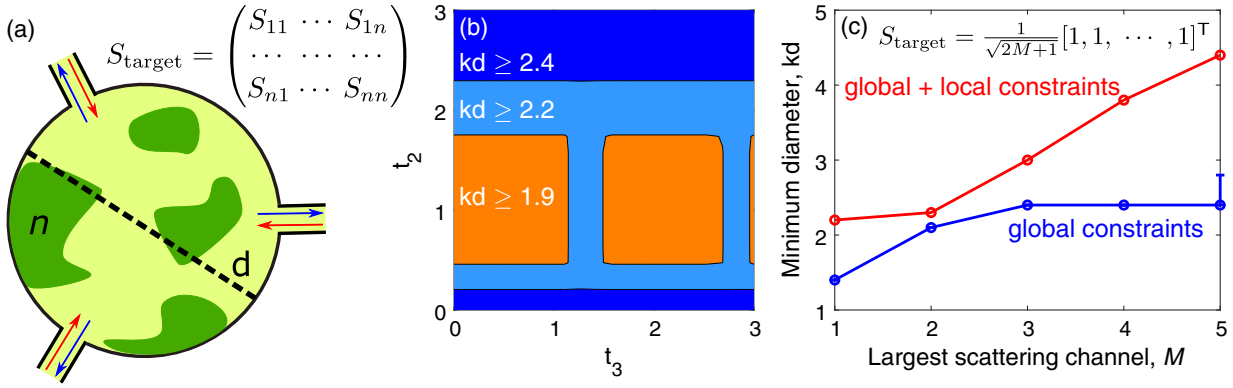

FIG. 2. (a) Photonic devices are often designed to achieve a specific "target" S matrix in a compact form factor. Our bounds enable identification of the minimum diameter d of any such device (relative to wave number k), for (b) nonuniform DFT matrix implementation (t_2 and t_3 are parameters of the DFT matrix) and (c) power splitters for a single input to $2M + 1$ outgoing channels. In (b), each point in the image represents a unique DFT matrix, and the colors indicate the minimum diameter for possibly achieving that scattering matrix. In (c) it is evident that local constraints are required to identify feasible design regions as the required functionality increases in complexity. In (b) and (c) the channels are TE cylindrical waves and the material has refractive index $n = \sqrt{12}$.

that can act as a DFT matrix if its diameter is smaller than that specified in Fig. 2(b). Thus our approach enables bounds on the minimal possible size of an optical element implementing specific functionality. A related calculation is shown in Fig. 2(c). In that case we consider a target S matrix for a power splitter, directing a single incident wave equally into outgoing spherical-wave channels index by m (where m is the angular index, $m = -M, \ldots, M$). We depict the minimum diameter as a function of the number of scattering channels, both for the global-constraint-only approach (blue) and our new approach with local constraints. (The error bar indicates a numerical instability in the global-constraint-only approach, cf. SM [53].) Whereas the global-constraint-only approach unphysically converges to wavelength scale as the number of channels increases, our new approach predicts an unavoidable increase in the diameter of the power splitter, representing the first such capability for capturing minimum-size increases with increasing complexity.

Far-field power–bandwidth limits.—The local-constraint bound framework resolves another outstanding question: how large can far-field scattering be over an arbitrary bandwidth $\Delta\omega$? In Ref. [15], bounds for near-field average-bandwidth response were derived using global constraints at a complex frequency, yet it was noted that the same technique fails in the far field (it exhibits an unphysical divergence). A feature of Eq. (2) is that the local conservation laws can also be applied at complex frequencies, as the inclusion of the conjugate frequency ω^* leads to operators that are positive semidefinite over the whole upper half of the complex-frequency plane, by passivity (cf. SM [53]).

A prototypical example to consider is the maximum extinction cross section $\sigma_{\text{ext}}(\omega)$ from a given material over a bandwidth $\Delta\omega$. Using contour-integral techniques from Refs. [15,78], the average extinction around a center frequency ω_0, over a bandwidth $\Delta\omega$, as measured by integration against a Lorentzian window function, $H(\omega) = \{[\Delta\omega/\pi]/[(\omega - \omega_0)^2 + \Delta\omega^2]\}$, can be written as the evaluation of a single scattering amplitude at a *complex* frequency $\tilde{\omega}$ (cf. SM [53]):

$$\begin{aligned}\langle\sigma_{\text{ext}}\rangle &= \int_{-\infty}^{+\infty} \sigma_{\text{ext}}(\omega) H(\omega) d\omega \\ &= \text{Im}[\tilde{\omega}\psi_{\text{inc}}^T(-\tilde{\omega})\phi(\tilde{\omega})], \end{aligned} \tag{7}$$

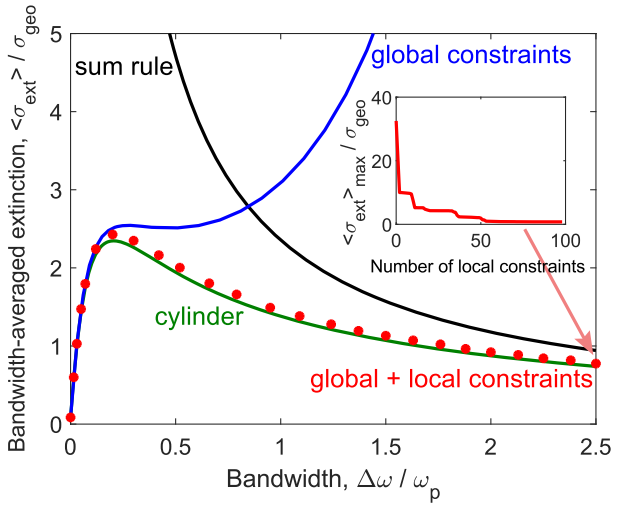

FIG. 3. Bounds on maximal bandwidth-averaged extinction, $\langle\sigma_{\text{ext}}\rangle_{\text{max}}$, as a function of bandwidth $\Delta\omega$ for a lossless Lorentz–Drude material with plasma frequency ω_p and oscillator frequency $\omega_c = 0.3015\omega_p$, which is chosen such that the permittivity is 12 at a center frequency $\omega_0 = 0.05\omega_p$. The bounds are normalized to the geometric cross section σ_{geo} of the designable region, a cylinder with diameter $d = 3/\omega_p$. While known sum rules (black) and global-constraint bounds (blue) are loose for many bandwidths, utilizing local constraints (convergence shown in inset) enables apparently tight bounds across all bandwidths.

where $\tilde{\omega} = \omega_0 + i\Delta\omega$. Equation (7) is a linear objective function of the form required by Eq. (4), evaluated at a complex frequency. By imposing the global and local conservation constraints at the complex frequency $\tilde{\omega}$, we can identify bounds to the bandwidth-averaged far-field response. Figure 3 shows the results of such a computation for a lossless Lorentz–Drude material (with plasma frequency ω_p) in a designable region with diameter $d = 3/\omega_p$. Included in the figure is a bound on average extinction from a known all-frequency sum rule [23,79] (black), which is descriptive in the infinite-bandwidth limit, and the global-constraint-only bounds (blue), which are useful in the small-bandwidth limit, but each diverges in the opposite limits. Through the use of global and local constraints (red), we can identify bounds over any bandwidth of interest, and we find that a cylindrical scatterer is nearly globally optimal.

Conclusions.—We have shown that local conservation laws enable computational bounds to light–matter interactions. The demonstrated bounds for optical analog computing and power–bandwidth limits are suggestive of a wide array of future possible applications. From the perspective of identifying feasible design volumes for target scattering matrices, a natural extension is to large-area, broadband metalenses. It is clear that there are trade-offs between diameter, bandwidth, and efficiency, but the optimal architecture and form factor is unknown. Our bounds may resolve the Pareto frontier. Similarly, the power–bandwidth limits have natural applications in photovoltaics [45,80–82] and ultrafast optics [83–85].

There are two key areas for improvement looking forward. The first is to nonlinear optics and nonlinear physics, where conservation laws analogous to Eq. (3) would not have the quadratic structure that enabled semidefinite-programming-based bounds here. The second is to identify faster computational schemes, such as those used in "fast solvers" [86–88], as the computational cost of semidefinite relaxations prohibited our exploration of structures far larger than wavelength scale. Overcoming both of these limitations would open interesting possibilities for applications ranging from quantum dynamics to large-scale metaoptics.

This work was supported by the Army Research Office under Grant No. W911NF-19-1-0279.

[1] J. S. Jensen and O. Sigmund, Topology optimization for nano-photonics, Laser Photonics Rev. **5**, 308 (2011).
[2] O. D. Miller, Photonic design: From fundamental solar cell physics to computational inverse design, Ph. D. thesis, University of California, Berkeley, 2012.
[3] M. P. Bendsoe and O. Sigmund, *Topology Optimization: Theory, Methods, and Applications* (Springer Science & Business Media, New York, 2013).
[4] S. Molesky, Z. Lin, A. Y. Piggott, W. Jin, J. Vucković, and A. W. Rodriguez, Inverse design in nanophotonics, Nat. Photonics **12**, 659 (2018).
[5] C. M. Lalau-Keraly, S. Bhargava, O. D. Miller, and E. Yablonovitch, Adjoint shape optimization applied to electromagnetic design, Opt. Express **21**, 21693 (2013).
[6] A. Y. Piggott, J. Lu, K. G. Lagoudakis, J. Petykiewicz, T. M. Babinec, and J. Vucković, Inverse design and demonstration of a compact and broadband on-chip wavelength demultiplexer, Nat. Photonics **9**, 374 (2015).
[7] K. Y. Yang, J. Skarda, M. Cotrufo, A. Dutt, G. H. Ahn, M. Sawaby, D. Vercruysse, A. Arbabian, S. Fan, A. Alù, and J. Vučković, Inverse-designed non-reciprocal pulse router for chip-based LiDAR, Nat. Photonics **14**, 369 (2020).
[8] N. V. Sapra, K. Y. Yang, D. Vercruysse, K. J. Leedle, D. S. Black, R. J. England, L. Su, R. Trivedi, Y. Miao, O. Solgaard, R. L. Byer, and J. Vučković, On-chip integrated laser-driven particle accelerator, Science **367**, 79 (2020).
[9] N. Yu and F. Capasso, Flat optics with designer metasurfaces, Nat. Mater. **13**, 139 (2014).
[10] F. Aieta, M. A. Kats, P. Genevet, and F. Capasso, Multiwavelength achromatic metasurfaces by dispersive phase compensation, Science **347**, 1342 (2015).
[11] S. Shrestha, A. C. Overvig, M. Lu, A. Stein, and N. Yu, Broadband achromatic dielectric metalenses, Light **7**, 85 (2018).
[12] A. Zhan, R. Gibson, J. Whitehead, E. Smith, J. R. Hendrickson, and A. Majumdar, Controlling three-dimensional optical fields via inverse Mie scattering, Sci. Adv. **5**, 1 (2019).
[13] C. E. Shannon and W. Weaver, *The Mathematical Theory of Communication* (University of Illinois Press, Urbana, IL, 1949).
[14] T. M. Cover, *Elements of Information Theory* (John Wiley & Sons, New York, 1999).
[15] H. Shim, L. Fan, S. G. Johnson, and O. D. Miller, Fundamental Limits to Near-Field Optical Response over Any Bandwidth, Phys. Rev. X **9**, 011043 (2019).
[16] H. B. Callen, *Thermodynamics and an Introduction to Thermostatistics* (John Wiley & Sons, New York, 1985).
[17] W. Shockley and H. J. Queisser, Detailed balance limit of efficiency of *p-n* junction solar cells, J. Appl. Phys. **32**, 510 (1961).
[18] D. J. Bergman, Bounds for the complex dielectric constant of a two-component composite material, Phys. Rev. B **23**, 3058 (1981).
[19] G. W. Milton, Bounds on the complex permittivity of a two-component composite material, J. Appl. Phys. **52**, 5286 (1981).
[20] G. W. Milton, *The Theory of Composites* (Cambridge University Press, Cambridge, England, 2002).
[21] H. A. Wheeler, Fundamental limitations of small antennas, Proc. IRE **35**, 1479 (1947).
[22] L. J. Chu, Physical limitations of omni-directional antennas, J. Appl. Phys. **19**, 1163 (1948).
[23] R. G. Gordon, Three sum rules for total optical absorption cross sections, J. Chem. Phys. **38**, 1724 (1963).
[24] E. M. Purcell, On the absorption and emission of light by interstellar grains, Astrophys. J. **158**, 433 (1969).

[25] B. H. J. Mckellar, M. A. Box, and C. F. Bohren, Sum rules for optical scattering amplitudes, J. Opt. Soc. Am. **72**, 535 (1982).
[26] C. Sohl, M. Gustafsson, and G. Kristensson, Physical limitations on broadband scattering by heterogeneous obstacles, J. Phys. A **40**, 11165 (2007).
[27] O. D. Miller, S. G. Johnson, and A. W. Rodriguez, Shape-Independent Limits to Near-Field Radiative Heat Transfer, Phys. Rev. Lett. **115**, 204302 (2015).
[28] J.-P. Hugonin, M. Besbes, and P. Ben-Abdallah, Fundamental limits for light absorption and scattering induced by cooperative electromagnetic interactions, Phys. Rev. B **91**, 180202(R) (2015).
[29] O. D. Miller, A. G. Polimeridis, M. T. H. Reid, C. W. Hsu, B. G. Delacy, J. D. Joannopoulos, M. Soljačić, and S. G. Johnson, Fundamental limits to optical response in absorptive systems, Opt. Express **24**, 3329 (2016).
[30] O. D. Miller, O. Ilic, T. Christensen, M. T. H. Reid, H. A. Atwater, J. D. Joannopoulos, M. Soljačić, and S. G. Johnson, Limits to the optical response of graphene and two-dimensional materials, Nano Lett. **17**, 5408 (2017).
[31] S. Sanders and A. Manjavacas, Analysis of the limits of the local density of photonic states near nanostructures, ACS Photonics **5**, 2437 (2018).
[32] Y. Yang, O. D. Miller, T. Christensen, J. D. Joannopoulos, and M. Soljačić, Low-loss plasmonic dielectric nanoresonators, Nano Lett. **17**, 3238 (2017).
[33] Y. Yang, A. Massuda, C. Roques-Carmes, S. E. Kooi, T. Christensen, S. G. Johnson, J. D. Joannopoulos, O. D. Miller, I. Kaminer, and M. Soljačić, Maximal spontaneous photon emission and energy loss from free electrons, Nat. Phys. **14**, 894 (2018).
[34] J. Michon, M. Benzaouia, W. Yao, O. D. Miller, and S. G. Johnson, Limits to surface-enhanced Raman scattering near arbitrary-shape scatterers, Opt. Express **27**, 35189 (2019).
[35] H. Zhang, C. W. Hsu, and O. D. Miller, Scattering concentration bounds: Brightness theorems for waves, Optica **6**, 1321 (2019).
[36] S. Molesky, W. Jin, P. S. Venkataram, and A. W. Rodriguez, T Operator Bounds on Angle-Integrated Absorption and Thermal Radiation for Arbitrary Objects, Phys. Rev. Lett. **123**, 257401 (2019).
[37] H. Shim, H. Chung, and O. D. Miller, Maximal Free-Space Concentration of Electromagnetic Waves, Phys. Rev. Applied **14**, 014007 (2020).
[38] H. Shim, Z. Kuang, and O. D. Miller, Optical materials for maximal nanophotonic response (Invited), Opt. Mater. Express **10**, 1561 (2020).
[39] S. Molesky, P. Chao, W. Jin, and A. W. Rodriguez, Global T operator bounds on electromagnetic scattering: Upper bounds on far-field cross sections, Phys. Rev. Research **2**, 033172 (2020).
[40] M. Gustafsson, K. Schab, L. Jelinek, and M. Capek, Upper bounds on absorption and scattering, arXiv:1912.06699.
[41] S. Molesky, P. S. Venkataram, W. Jin, and A. W. Rodriguez, Fundamental limits to radiative heat transfer: Theory, Phys. Rev. B **101**, 035408 (2020).
[42] Z. Kuang, L. Zhang, and O. D. Miller, Maximal single-frequency electromagnetic response, arXiv:2002.00521.
[43] G. Angeris, J. Vuckovic, and S. P. Boyd, Computational bounds for photonic design, ACS Photonics **6**, 1232 (2019).
[44] R. Trivedi, G. Angeris, L. Su, S. Boyd, S. Fan, and J. Vuckovic, Fundamental bounds for scattering from absorptionless electromagnetic structures, Phys. Rev. Applied **14**, 014025 (2020).
[45] Z. Yu, A. Raman, and S. Fan, Fundamental limit of nanophotonic light trapping in solar cells, Proc. Natl. Acad. Sci. U.S. A. **107**, 17491 (2010).
[46] F. Presutti and F. Monticone, Focusing on bandwidth: Achromatic metalens limits, Optica **7**, 624 (2020).
[47] H. Chung and O. D. Miller, High-NA achromatic metalenses by inverse design, Opt. Express **28**, 6945 (2020).
[48] M. Laurent and F. Rendl, Semidefinite programming and integer programming, Handbooks Oper. Res. Manag. Sci. **12**, 393 (2005).
[49] Z. Q. Luo, W. K. Ma, A. So, Y. Ye, and S. Zhang, Semidefinite relaxation of quadratic optimization problems, IEEE Signal Process. Mag. **27**, 20 (2010).
[50] J. D. Jackson, *Classical Electrodynamics*, 3rd ed. (John Wiley & Sons, New York, 1999).
[51] R. G. Newton, Optical theorem and beyond, Am. J. Phys. **44**, 639 (1976).
[52] D. R. Lytle, P. S. Carney, J. C. Schotland, and E. Wolf, Generalized optical theorem for reflection, transmission, and extinction of power for electromagnetic fields, Phys. Rev. E **71**, 056610 (2005).
[53] See Supplemental Material at http://link.aps.org/supplemental/10.1103/PhysRevLett.125.263607 for the mathematical formulation of the constraints and objectives for the optimization problem, which includes Refs. [54–61].
[54] W. C. Chew, M. S. Tong, and B. Hu, Integral equation methods for electromagnetic and elastic waves, Synth. Lect. Comput. Electromagn. **3**, 1 (2008).
[55] A. Ben-Tal and M. Teboulle, Hidden convexity in some nonconvex quadratically constrained quadratic programming, Math. Program. **72**, 51 (1996).
[56] J. Park and S. Boyd, General heuristics for nonconvex quadratically constrained quadratic programming, arXiv:1703.07870.
[57] L. D. Landau and E. M. Lifshitz, *Electrodynamics of Continuous Media* (Pergamon Press, New York, 1960).
[58] H. M. Nussenzveig, *Causality and Dispersion Relations* (Academic Press, New York, 1972).
[59] A. H. Zemanian, The Hilbert port, SIAM J. Appl. Math. **18**, 98 (1970).
[60] A. H. Zemanian, *Realizability Theory for Continuous Linear Systems* (Courier Corporation, New York, 1995).
[61] A. Welters, Y. Avniel, and S. G. Johnson, Speed-of-light limitations in passive linear media, Phys. Rev. A **90**, 023847 (2014).
[62] J.-M. Jin, *Theory and Computation of Electromagnetic Fields* (John Wiley & Sons, New York, 2011).
[63] S. Boyd and L. Vandenberghe, *Convex Optimization* (Cambridge University Press, Cambridge, England, 2004).
[64] L. Vandenberghe and S. Boyd, Semidefinite programming, SIAM Rev. **38**, 49 (1996).
[65] M. X. Goemans and D. P. Williamson, Improved approximation algorithms for maximum cut and satisfiability

problems using semidefinite programming, J. ACM **42**, 1115 (1995).
[66] Peng Hui Tan and L. Rasmussen, The application of semidefinite programming for detection in CDMA, IEEE J. Sel. Areas Commun. **19**, 1442 (2001).
[67] P. Biswas, T. C. Lian, T. C. Wang, and Y. Ye, Semidefinite programming based algorithms for sensor network localization, ACM Trans. Sens. Networks **2**, 188 (2006).
[68] A. B. Gershman, N. D. Sidiropoulos, S. Shahbazpanahi, M. Bengtsson, and B. Ottersten, Convex optimization-based beamforming, IEEE Signal Process. Mag. **27**, 62 (2010).
[69] A. Silva, F. Monticone, G. Castaldi, V. Galdi, A. Alu, and N. Engheta, Performing mathematical operations with metamaterials, Science **343**, 160 (2014).
[70] A. Pors, M. G. Nielsen, and S. I. Bozhevolnyi, Analog computing using reflective plasmonic metasurfaces, Nano Lett. **15**, 791 (2015).
[71] T. Zhu, Y. Zhou, Y. Lou, H. Ye, M. Qiu, Z. Ruan, and S. Fan, Plasmonic computing of spatial differentiation, Nat. Commun. **8**, 1 (2017).
[72] H. Kwon, D. Sounas, A. Cordaro, A. Polman, and A. Alù, Nonlocal Metasurfaces for Optical Signal Processing, Phys. Rev. Lett. **121**, 173004 (2018).
[73] N. M. Estakhri, B. Edwards, and N. Engheta, Inverse-designed metastructures that solve equations, Science **363**, 1333 (2019).
[74] E. M. Purcell and C. R. Pennypacker, Scattering and Absorption of Light by Nonspherical Dielectric Grains, Astrophys. J. **186**, 705 (1973).
[75] B. T. Draine and P. J. Flatau, Discrete-dipole approximation for scattering calculations, J. Opt. Soc. Am. A **11**, 1491 (1994).
[76] G. Strang, Wavelets, Am. Sci. **82**, 250 (1994).
[77] K. R. Rao, D. N. Kim, and J. J. Hwang, Nonuniform DFT, in *Fast Fourier Transform-Algorithms and Applications* (Springer Science & Business Media, 2011).
[78] H. Hashemi, C.-W. Qiu, A. P. McCauley, J. D. Joannopoulos, and S. G. Johnson, Diameter-bandwidth product limitation of isolated-object cloaking, Phys. Rev. A **86**, 013804 (2012).
[79] Z. J. Yang, T. J. Antosiewicz, R. Verre, F. J. Garcia De Abajo, S. P. Apell, and M. Kall, Ultimate limit of light extinction by nanophotonic structures, Nano Lett. **15**, 7633 (2015).
[80] V. Ganapati, O. D. Miller, and E. Yablonovitch, Light trapping textures designed by electromagnetic optimization for subwavelength thick solar cells, IEEE J. Photovoltaics **4**, 175 (2014).
[81] S. Buddhiraju and S. Fan, Theory of solar cell light trapping through a nonequilibrium Green's function formulation of Maxwell's equations, Phys. Rev. B **96**, 035304 (2017).
[82] M. Benzaouia, G. Tokic, O. D. Miller, D. K. P. Yue, and S. G. Johnson, From Solar Cells to Ocean Buoys: Wide-Bandwidth Limits to Absorption by Metaparticle Arays, Phys. Rev. Applied **11**, 034033 (2019).
[83] A. Weiner, *Ultrafast Optics* (John Wiley & Sons, New York, 2011), Vol. 72.
[84] G. P. Agrawal, *Nonlinear Fiber Optics*, 5th ed. (Academic Press, New York, 2013).
[85] F. Wang, A. G. Rozhin, V. Scardaci, Z. Sun, F. Hennrich, I. H. White, W. I. Milne, and A. C. Ferrari, Wideband-tuneable, nanotube mode-locked, fibre laser, Nat. Nanotechnol. **3**, 738 (2008).
[86] V. Rokhlin, Rapid solution of integral equations of classical potential theory, J. Comput. Phys. **60**, 187 (1985).
[87] R. F. Harrington, *Field Computation by Moment Methods* (Wiley-IEEE Press, New York, 1993).
[88] S. G. Johnson and J. D. Joannopoulos, Block-iterative frequency-domain methods for Maxwell's equations in a planewave basis, Opt. Express **8**, 173 (2001).